Joachim Wosnitza

Fermi Surfaces of Low-Dimensional Organic Metals and Superconductors

With 88 Figures

Springer

Dr. Joachim Wosnitza
Physikalisches Institut
Universität Karlsruhe
Engesserstraße 7
D-76128 Karlsruhe

Cataloging-in-Publication Data applied for

Die Deutsche Bibliothek - CIP-Einheitsaufnahme

Wosnitza, Joachim:
Fermi surfaces of low dimensional organic metals and superconductors / Joachim Wosnitza. - Berlin ; Heidelberg ; New York ; Barcelona ; Budapest ; Hong Kong ; London ; Milan ; Paris ; Santa Clara ; Singapore ; Tokyo : Springer, 1996
(Springer tracts in modern physics ; Vol. 134)
ISBN 3-540-60674-2
NE: GT

Physics and Astronomy Classification Scheme (PACS):
71.25.Hc, 74.70.Kn, 75.30.Fv

ISBN 3-540-60674-2 Springer-Verlag Berlin Heidelberg New York

Typesetting: Camera-ready copy from the author using a Springer TEX macro-package
Cover design: Springer-Verlag, Design & Production
SPIN: 10511697 56/3144-5 4 3 2 1 0 – Printed on acid-free paper

Preface

The activities in the synthesis and investigation of organic metals were originally initiated three decades ago by the proposal of polymeric superconductors with extraordinary high transition temperatures. The extensive research finally succeeded in the discovery of highly conducting organic metals that showed superconductivity. However, this superconductivity was at rather low temperatures and in the beginning occurred only under high pressure. Although the mechanism responsible for the superconductivity in the organic compounds known to date has nothing to do with the originally proposed excitonic interaction, the physical properties of these low-dimensional materials show a fascinating variety of unusual and exciting effects.

The metallic and superconducting states of these organic compounds are highly sensitive to external parameters such as the pressure, magnetic field, and cooling rate. By proper treatment the metallic state may be suppressed *and charge* or spin density wave states, antiferromagnetism or weak ferromagnetism, can easily be induced or destroyed. Sometimes even a coexistence of these contradictory states appears to be possible.

A key for a better understanding of organic metals is the knowledge of the electronic structure, i. e., the Fermi surface. The most direct and, therefore, most important tools for the experimental determination of the Fermi surface are the de Haas–van Alphen (dHvA) and Shubnikov–de Haas (SdH) effects. These methods, which were already fully developed in the late 1950s, have undergone a great revival in recent years, stimulated in particular through the success in resolving the Fermi-surface topology in organic superconductors.

In this review an introduction to the structural, electronic, and superconducting properties and a comprehensive overview of the present-day knowledge of the Fermi surfaces of organic low-dimensional metals will be given. Thereby, attention is focused mainly on the quasi two-dimensional charge transfer salts, whereas the quasi one-dimensional organic metals are reviewed in a somewhat shorter fashion. The recently discovered three-dimensional fullerenes based on C_{60} are excluded altogether in this overview, especially because to date only very limited experimental data concerning the Fermi surfaces are available.

The material is presented in five chapters. After the mainly historical background given in the introduction in Chap. 1 an outline of the basic

structural, electronic, and superconducting properties is presented in Chap. 2. Chapter 3 gives a brief introduction to the theoretical understanding of magnetic quantum oscillations and angular dependent magnetoresistance oscillations. The experimental results are discussed in detail in Chap. 4. Finally, Chap. 5 gives some concluding remarks and an outlook of future developments.

New results and new materials are appearing constantly in this highly topical field of the "fermiology of organic superconductors and metals". Therefore, this review can give only a picture of the subject as it currently is. In the forthcoming years many of the present-day questions may be solved, whereas certainly other new aspects of solid-state properties might occur.

Finally it is a pleasure to thank the following people who have contributed to this work in different ways: first of all, Prof. H. von Löhneysen, whose continuous interest, encouragement and discussions motivated the work considerably; Prof. G. Crabtree, Drs. U. Welp, and W. Kwok for initiating the interest in the experimental technique of dHvA measurements, for their sharing of experimental knowledge, and for many fruitful discussions; Prof. J. Williams, Drs. H. Wang, D. Carlson, and U. Geiser for sharing their crystals and their knowledge about organic metals; Prof. D. Schweitzer for his spontaneous and continuous support with high-quality crystals and for many discussions; Drs. N. D. Kushch, H. Müller, and J. Schlueter for the supply of crystals; Drs. W. Biberacher, J. S. Brooks, M. Dressel, T. Ishiguro, M. Kartsovnik, M. Kund, M. Lang, V. N. Laukhin, T. Sasaki, and Y. Sushko for many useful discussions; N. Herrmann, D. Beckmann, S. Wanka, Dr. G. Goll, and Dr. X. Liu for their large contributions to many of the experimental results presented here; Profs. E. Dormann and P. Wölfle for valuable suggestions improving the final state of this review; finally the many colleagues who allowed the publication of their results and supplied information prior to publication.

Karlsruhe, January 1996 *Joachim Wosnitza*

1. Introduction

Usually organic materials are regarded as being prototypes of electrical insulators. In everyday life a vast set of different carbon-based substances, such as fibers, coatings, synthetic rubbers, plastic bags and so on, surround us. However, some of the organic compounds showed at least at room temperature metallic conductivity, i. e., decreasing resistivity with decreasing temperature. These "synthetic metals", however, usually have conductivities orders of magnitude less than Cu. On the other hand, the technology in the synthesis of organic materials is well developed and there is a unique possibility in tailoring solid state compounds with the desired mechanical, electrical and even magnetic properties. However, it appears that the interactions governing these properties are very subtle and to date we are still far from achieving the "molecular engineering" of substances with desired electronic and magnetic properties.

The first organic compounds which showed electronic conductivity at room temperature were semiconductors [1]. Much effort was spent on the synthesis of materials with higher conductivity. An important step in the development of organic metals was the discovery of TTF–TCNQ [2] consisting of the organic electron acceptor tetracyano-p-quinodimethane (TCNQ) and the electron donor tetrathiafulvalene (TTF). This material exhibits a metallic conductivity, σ, along the stacking direction with $\sigma \approx 10^4\,\mathrm{S\,cm^{-1}}$ near 60 K (Cu has $\sim 10^6\,\mathrm{S\,cm^{-1}}$ at room temperature). Below this temperature, however, a Peierls metal–insulator transition [3] occurs and the conduction electrons no longer contribute to the conductivity. As will be discussed in more detail in Sect. 2.2.3, Fröhlich has pointed out that a one-dimensional (1D) metal in principle is unstable against a lattice distortion and a concomitant gap opening at the Fermi level [4]. Indeed, in many quasi-1D organic conductors the ground state is characterized by collective ordering phenomena like charge density wave (CDW) or spin density wave (SDW) states [5]. Numerous investigations deal with organic systems showing these Peierls transitions in order to get a better understanding of the nature of this low-temperature ground state. Apart from the 1D materials with TTF other charge transfer salts based on so-called arenes, such as pyrene, perylene, or fluoranthene [6], are well-studied Peierls systems.

The 1D and possibly even 2D metals are also especially interesting, namely the theoretically predicted occurrence of a Luttinger liquid [7]. For example, the experimental search for the expected behavior of a Luttinger liquid peaked after the finding of quasi 1D TTF–TCNQ. Recently, photoemission data of a 1D and some 2D organic metals revealed one of the features of a Luttinger liquid, namely the missing of a sharp Fermi edge [8, 9, 10]. Up to now, however, it is not clear whether the low-dimensional organic conductors can be described within the Luttinger picture.

Since the beginning of the investigations of organic metals the search for superconductivity was one of the main goals. This was especially stimulated by a hypothesis made by Little [11] that in organic polymers with highly polarizable side chains the pairing of electrons to Cooper pairs should be highly favorable. This, he argued, could result in extremely high superconducting transition temperatures because the region of positive charge generating the attractive interaction is caused by the displacement of an electron with much smaller mass than that of the moving ions constituting a lattice vibration in inorganic superconductors. However, as should be stated here clearly, in spite of the large efforts spent so far no superconductivity based on the exitonic mechanism proposed by Little has yet been found.

The first organic superconductor discovered in 1979, 15 years after Little's stimulating idea, was $(TMTSF)_2PF_6$ [12], where TMTSF stands for tetramethyltetraselenafulvalene. At ambient pressure, however, this material shows a metal–insulator transition to a low temperature state which has been recognized as a SDW phase. Only with the application of the considerably large pressure of $\sim 12\,\mathrm{kbar}$ can this phase be suppressed and superconductivity with a transition temperature of $T_c \approx 0.9\,\mathrm{K}$ occur. Shortly afterwards a series of isostructural superconductors obtained simply by replacing the charge-compensating anion PF_6 by AsF_6, SbF_6, TaF_6, ReO_4, FSO_3, and ClO_4 were discovered [13]. Of all these materials, however, only $(TMTSF)_2ClO_4$ is a superconductor ($T_c \approx 1.4\,\mathrm{K}$) at ambient pressure [14].

Apart from these so-called Bechgaard salts based on TMTSF, a large variety of organic superconductors with different building blocks were found within the next few years. Figure 1.1 shows the principal molecules of more than 60 different organic superconductors known to date [13]. The largest number of superconductors is based on the molecule BEDT–TTF (bisethylenedithio-tetrathiafulvalene or ET for short). The first superconducting material based on ET was $(ET)_2(ReO_4)_2$ [15]. This compound also needs pressure (4.5 kbar) to suppress an insulating state and allow superconductivity at $T_c \approx 2\,\mathrm{K}$. The organic charge transfer salt with the highest T_c to date (besides the fullerenes) is also based on the ET molecule. κ-$(ET)_2Cu[N(CN)_2]Cl$ has a very complicated low-temperature phase diagram but shows superconductivity at $T_c \approx 12.8\,\mathrm{K}$ with only moderate pressure of 0.3 kbar [16]. So far at least 30 different ET-based superconductors are

known, many of them at ambient pressure with transition temperatures up to $\sim 11.6\,\mathrm{K}$.

In contrast to the Bechgaard salts which are quasi-1D, the ET materials are characterized by their two-dimensional (2D) electronic structure. In both salts the electronic bands are formed by the overlapping molecular π orbitals. Along certain directions the distances between either Se–Se or S–S is less than the van der Waals radii of 3.96 Å or 3.6 Å, respectively. Within the ET compounds many different ways of stacking of the ET molecules is possible. These polymorphic phases are denoted by α, β, κ, θ, etc. and will be discussed in Sect. 2.3.1.

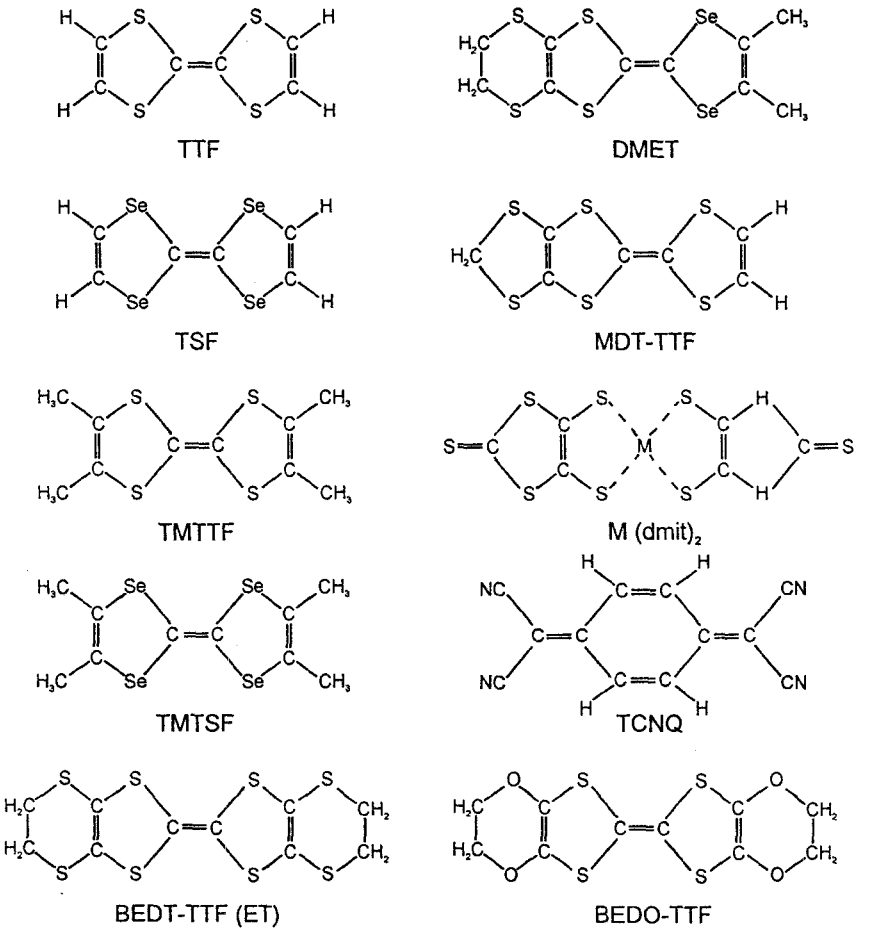

Fig. 1.1. Molecular structures of some building blocks in organic conductors and superconductors

Other organic superconductors are based on DMET (dimethyl-ethylene-dithio-diselenedithiafulvalene), an asymmetric molecule hybridized from ET and TMTSF [17]. According to its origin the physical properties are somewhere between one and two dimensional. Also based on asymmetric donors are the ambient-pressure superconductors $(MDT\text{–}TTF)_2AuI_2$ with $T_c \approx 3.5\,K$ [18] and $(DMET\text{–}TSeF)_2X$ with $X = AuI_2$ and I_3 (T_c below 1 K), where MDT–TTF stands for methylenedithio-TTF and DMET–TSeF for dimethyl-ethylenedithio-tetraselenafulvalene [19].

According to the BCS theory T_c is to a first approximation proportional to the Debye temperature $\Theta_D \propto \mu^{-1/2}$, where μ might be related to the reduced molecular weight. Therefore, a main goal was the reduction of the molecular weight of the organic constituents. Indeed, two organic superconductors based on the molecule BEDO–TTF (bisethylenedioxy-TTF), where the outer S atoms in ET are substituted by O, have been synthesized. Contrary to expectations, however, the transition temperatures are relatively low around 1 K [20, 21].

Furthermore, superconductivity has been found in some salts based on the acceptor molecule $M(dmit)_2$, where M = Ni, Pd, or Pt and dmit is 4,5-dimercapto-1,3-dithiole-2-thione (= C_3S_5) [22, 23].

The properties of organic metals both in the superconducting and the metallic states are quite unusual. The low-temperature state is highly sensitive to external parameters like pressure, field or cooling rate. This manifests itself in very rich phase diagrams, where superconductivity, CDW, SDW and even ferromagnetism exist next to each other. Many of the organic superconductors show an extraordinarily large change of T_c with pressure. Some of the synthetic metals have ground states under ambient conditions which can be easily modified under moderate pressure. This results, for example, in two largely different superconducting transition temperatures in β-$(ET)_2I_3$ or under certain conditions in reentrant superconductivity in κ-$(ET)_2Cu[N(CN)_2]Cl$.

To date the nature of the superconducting state in organic metals is controversial and either BCS or unconventional behavior has been suggested. Experimental data are not yet conclusive and are interpreted in both ways. The missing of the Hebel-Slichter peak at T_c and the observation of a peak at lower temperatures in some NMR experiments were interpreted as a sign of unusual behavior. This and the existence of antiferromagnetic ordering and superconductivity close to each other in TMTSF and also in some ET salts are sometimes taken to suggest an electron pairing mechanism due to spin fluctuations [24, 25]. On the other hand, tunneling, magnetization, and specific-heat data are consistent with the usual electron–phonon coupling with a tendency, however, towards strong coupling. Since the low-dimensional organic superconductors behave in many aspects similar to the layered cuprate high-T_c superconductors the same mechanism principle might be responsible for the occurrence of superconductivity. In the latter materials some experimental

evidence points to a non-Fermi liquid-like behavior with, however, a well-defined Fermi surface. To account for this apparent contradiction, therefore, the concept of spin-charge separation resulting in a Luttinger liquid has been proposed [26]. However, the actual relevance of the Luttinger-liquid picture to 2D organic superconductors is unclear and remains controversial. Many other mechanisms for superconductivity in organic metals, such as electron-molecular vibration interaction, so-called "g-ology" [27], excitonic models, and so on, have been discussed [25]. An excellent introduction to these different theories and to the physics of organic superconductors is given by Ishiguro and Yamaji [28].

One important point understanding metallic and superconducting behavior is that of the Fermi surface (FS). The key tools for mapping out the FS topology are measurements of the de Haas–van Alphen (dHvA) and Shubnikov–de Haas (SdH) effect. Of course, these magnetic quantum oscillations are only observable if a closed extremal orbit of the charge carriers in $\boldsymbol{k}$ space exists. Therefore, in 1D material with only open FS sheets the observation of dHvA or SdH oscillations is not possible. However, in the quasi 1D organic metals $(TMTSF)_2X$, where X stands for the charge-compensating anion, other unexpected effects in high magnetic fields of different origin have been observed. These were, for example, the field-induced SDW state, giant angular dependent magnetoresistance oscillations (AMRO), and the so-called rapid oscillations. These findings have stimulated enormous efforts both experimentally and theoretically, where new models have been developed clarifying some of the observed peculiarities. To date, however, many open questions still exist, challenging both experimental and theoretical studies to clarify the remaining problems. In Sects. 2.2 and 4.1 some of these basic features of the 1D organic metals will be reviewed.

The 2D organic conductors, on the other hand, are ideally suited for the observation of both dHvA and SdH effects. With the increasing quality of the samples first SdH oscillations in κ-$(ET)_2Cu(NCS)_2$ [29] and β-$(ET)_2IBr_2$ [30] were discovered in 1988. In the following years magnetic quantum oscillations in many other organic metals were found [31]. These investigations made a considerable contribution to understanding the electronic properties of organic charge transfer salts. For many compounds it was possible to map out the exact topology of the FS which allowed a direct comparison with the predictions of band-structure calculations. Very often a remarkable agreement between experiment and the calculated FS was found. In these calculations the FS was obtained by the tight-binding Hückel method under rather crude approximations.

All the ET compounds are characterized by their nearly perfect 2D band structure resulting in an almost cylindrical form of the FS. For some materials it was possible to determine quantitatively the transfer integral between the ET layers, i. e., the dispersion of the energy-momentum relation perpendicular to the highly conducting planes, the so-called warping. In some cases an

extremely 2D band structure was found which resulted in very unusual features such as giant amplitudes and a strong harmonic content of the magnetic quantum oscillations. Other ET salts with additional 1D open FS topologies have been found to be unstable against a SDW transition. This leads to peculiar, unexpected and still not quite understood behavior in SdH and dHvA measurements.

Both 1D and 2D organic metals are, of course, three-dimensional crystals with a certain degree of three-dimensionality also in the electronic system. This results in a corrugated form of the FS which gives rise to a distinct kind of AMRO. Therefore, measurements of the angular dependence of the resistance in magnetic fields has become a new and powerful tool to determine principal features of low-dimensional band structures. Section 3.3 will give a brief introduction into the present understanding of the AMRO in quasi 1D and 2D metals.

In recent years successful measurements of magnetic quantum oscillations have been employed to uncover the nature of the low-temperature states in organic metals. SdH measurements under pressure show the changes of the band-structure due to the increasing dimensionality. The observation of dHvA oscillations in the superconducting state was possible so far in one ET salt [32] and gave more insight into the kind of scattering mechanism of the quasiparticles in the Shubnikov phase.

From the temperature dependence of the dHvA (or SdH) oscillations it is possible to extract the effective cyclotron mass (see Sect. 3.1). Comparisons of the mass obtained by these measurements with values from band-structure calculations, cyclotron resonance and specific-heat measurements are sometimes inconsistent. Whether strong electron–electron or electron–phonon interactions play the dominant role for this discrepancy is still under considerable debate and further studies have to deal with this question. Chapter 4 will review the present-day knowledge of the highly active field of "the fermiology of organic superconductors".

2. Some Principal Properties

2.1 Synthesis

Several review articles and a comprehensive book already exist which describe the detailed synthesis of the miscellaneous organic donor molecules and the experimental procedures to obtain organic conducting salts [33]. Therefore, only a few introductory remarks concerning the principal crystal growth technique will be given here.

The usual method of producing high-quality single crystals is a process called "electrocrystallization", during which the organic electron donor molecules are oxidized electrochemically. In the same process crystals are built with the charge-balancing anions. Typically, an H-configuration cell with an ultrafine porosity glass frit and two platinum electrodes is used for the crystal growing. The donor molecules, e. g., TMTSF or ET with an appropriate solvent, are put inside the anode compartment. A supporting electrolyte, e. g., NBu_4X, is added both to the anode and cathode compartment, where Bu is n-butyl and X is the desired monovalent anion such as ClO_4^- or $Cu(NCS)_2^-$. Electrocrystallization is a slow process which takes typically from one week up to a few months. The current density is kept at the lowest possible level ($\sim 1\,\mu A/cm^2$) to initiate crystal growth. After seed crystals appear the current density is reduced further to avoid the generation of divalent donor cations and to obtain large single crystals. Sometimes after harvesting the first batch of crystals a second and third growth process in used solution results in higher quality crystals. Usually, the crystals obtained are black. The quasi 1D materials have a needle-like form with the long axis of a few millimeter length being the highly conducting one. The 2D salts have plate-like shapes of a few millimeter side length and smaller thickness perpendicular to the highly conducting planes of a few tenths of a millimeter.

To obtain the many different phases of the metals based on ET donor molecules, the exact current density, the right solvent, and the correctly prepared starting material are essential. The ET-I_3 system, for example, has more than a dozen different phases with different stoichiometry [34]. For the usual charge transfer with the formula $(ET)_2I_3$ six phases are known, some of which can be converted from the crystals already grown by a special heat and pressure treatment.

Considerable effort is currently being spent on the improvement of crystal qualities and the evaluation of specific growth conditions to obtain the reliable crystallographic phases required. Consequently, the number of new organic metals is growing steadily. Often for many of these salts only the structural parameters and a few physical properties are investigated. Superconducting species, however, are attracting greater attention and are studied more carefully.

2.2 Quasi One-Dimensional Systems

This section gives a brief description of the crystal structure, the electronic properties and the superconductivity of the so-called Bechgaard salts with the general formula $(TMTSF)_2X$, where X represents a monovalent anion [35]. $(TMTSF)_2PF_6$ was the first organic compound which showed superconductivity [12]. This discovery has boosted an enormous amount of activity, resulting in a whole family of superconducting compounds all based on TMTSF. The isomorphous $(TMTTF)_2X$ salts, on the other hand, do not show superconductivity.[1] The building block tetramethyltetrathiafulvalene differs from TMTSF only in the substitution of S atoms instead of the four Se atoms (Fig. 1.1). The sulfur-based charge transfer salts, however, show a shallow minimum in the resistivity at $\sim 200\,\mathrm{K}$ and are semiconducting at lower temperatures [37]. Besides their intensively investigated and sometimes unusual superconducting properties the 1D organic materials served as model systems for the study of spin-Peierls and SDW transitions. Since in the (P, T) phase diagram these transitions occur in the vicinity of superconductivity it is speculated that magnetic ordering is related to the mechanism for superconductivity.

2.2.1 Crystal Structure of $(TMTSF)_2X$

The structure of tetramethyltetraselenafulvalene $[=(CH_3)_4C_6Se_4]$ is shown in Fig. 1.1. TMTSF is a planar brick-like molecule. In the charge transfer salts $(TMTSF)_2X$ these bricks are stacked in columns with a slight tendency towards dimerization. As an example, two views of the crystal structure of $(TMTSF)_2PF_6$ are shown in Fig. 2.1 [38]. The columns are formed along the a axis which is also the axis with the highest electrical conductivity. The anions, here PF_6^-, are located between these columns. The crystal symmetry is triclinic with space group $P\bar{1}$. The lattice parameters at room temperature for the cell containing one chemical formula unit (Z=1) are $a = 7.297\,\text{Å}$, $b = 7.711\,\text{Å}$, $c = 13.522\,\text{Å}$, $\alpha = 83.39°$, $\beta = 86.27°$, and $\gamma = 71.01°$.

[1] Recently some indications for superconductivity in $(TMTTF)_2Br$ have been found at pressures of 26 kbar [36]. See Sect. 2.2.3.

Two TMTSF molecules transfer one electron to PF_6^-. This monovalent electron acceptor can be replaced by AsF_6^-, SbF_6^-, and TaF_6^-, all with octahedral symmetry and superconducting transition temperatures in the compound of $\sim 1\,\mathrm{K}$ under applied pressures of $\sim 10\,\mathrm{kbar}$. The anions with tetra-

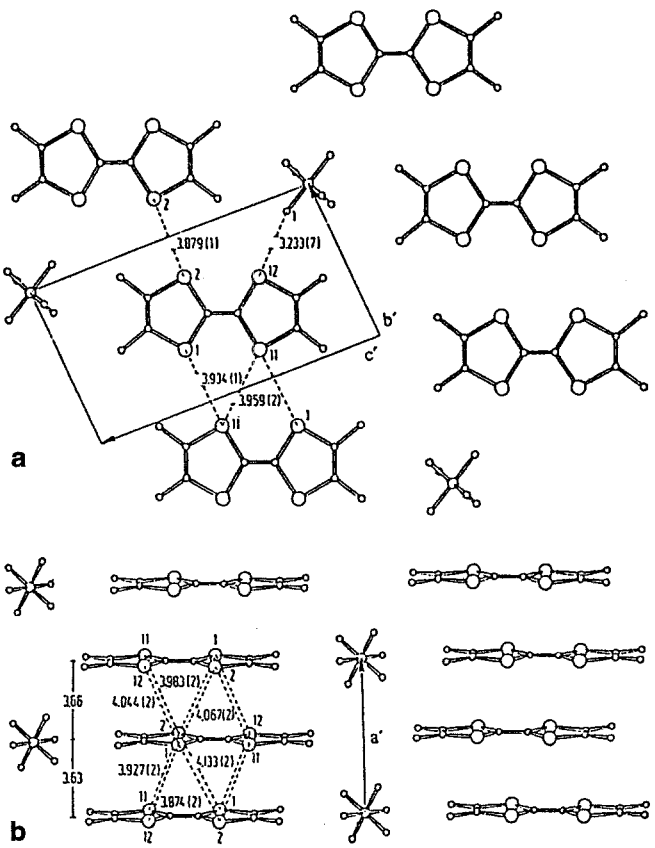

Fig. 2.1. (a) Crystal structure of $(TMTSF)_2PF_6$ viewed along the a direction and (b) 10° tilted side view of the TMTSF stacks. a', b', and c' are the projections of a, b, and c. The distances are in Å. From [38]

hedral symmetry, ClO_4^- and ReO_4^-, keep the crystal structure isomorphous. $(TMTSF)_2ClO_4$ is the only quasi-1D metal which becomes superconducting under ambient pressure [14]. The acceptor X can further be replaced by a large variety of other anions some containing even magnetic constituents such as $FeCl_4^-$ [39]. However, the only other superconducting Bechgaard salt found to date is $(TMTSF)_2FSO_3$ with the highest T_c of this family at $\sim 3\,\mathrm{K}$ [40]. Salts containing the electron donor TMTTF form isomorphous structures but become insulating at lower temperatures. The compounds $(TMTTF)_2X$ are, therefore, well suited for comparative studies between isostructural su-

perconductors and insulators. Section 2.2.3 discusses the reasons which are believed to be responsible for the electronic differences observed.

2.2.2 Electronic Structure

In Fig. 2.1 the most important intermolecular Se–Se distances are given [38]. As can be seen from this figure, the spacings of the Se atoms are around 3.9 Å both along the stacking direction and in the perpendicular plane. This value is approximately the sum of the van der Waals radii of the Se atoms, 3.96 Å. Although the distances within and perpendicular to the stacks are almost the same in $(TMTSF)_2X$ the overlap is strongest within the columns. This is due to the fact that between two neighboring planar TMTSF molecules only two Se atoms are in side-by-side contact. In the stacking direction, on the other hand, four Se orbitals are overlapping. In addition, the overlap is made by π-electron orbitals which extend in the stacking direction. This kind of overlap enables large electron transfers along the stacks, less coupling along the b direction, and the weakest transfer integrals along the c direction where the anions and the terminal methyl groups act as a barrier.

The calculation of the exact band structure from first principles, however, is rather complex and requires considerable simplifications. The usual and very successful method to calculate the band structure of organic charge transfer salts is a tight-binding method, called extended Hückel approximation. In this approximation, one starts from the molecular orbitals (MO) which are approximated by linear combinations of the constituent atomic orbitals. Each MO can be occupied by two electrons with antiparallel spins. These valence electrons are assumed to be spread over the whole molecule. Usually, only the highest occupied molecular orbital (HOMO) and the lowest unoccupied molecular orbital (LUMO) are relevant and are, therefore, considered in most band-structure calculations [41].

The principal properties of the low-dimensional organic metals, however, can be sketched already by the simple free-electron approximation, although here the delocalization of the π electrons is overestimated. Without any interaction in one dimension the electron energy levels are just given by $\epsilon(\boldsymbol{k}) = (\hbar^2/2m)k_a^2$, where m is the free-electron mass and k_a is the electron wave vector in the direction of highest conductivity. This dispersion relation in the repeated zone scheme is shown by the dashed lines in Fig. 2.2a. Inclusion of the correction of the free-electron parabola due to Bragg reflection at $\pm\pi/a$ gives the dispersion depicted as the solid lines in Fig. 2.2a. The available electrons have to be filled into the possible energy levels. Since in $(TMTSF)_2X$ each TMTSF has transferred half an electron to the anion X the highest band is filled to three-quarters. This results in a Fermi energy ϵ_F within the HOMO and the material should behave metallicly. Indeed, the $(TMTSF)_2X$ salts are metallic at room temperature. The overlap of the electronic wave functions in the other directions is very weak and, therefore, the

energy $\epsilon(\boldsymbol{k})$ is nearly independent of k_b and k_c. Figure 2.2b shows schematically the resultant 3D FS which consists of two almost parallel sheets perpendicular to k_a. Without any overlap along the b and c direction the sheets would be exactly parallel as shown by the dashed lines.

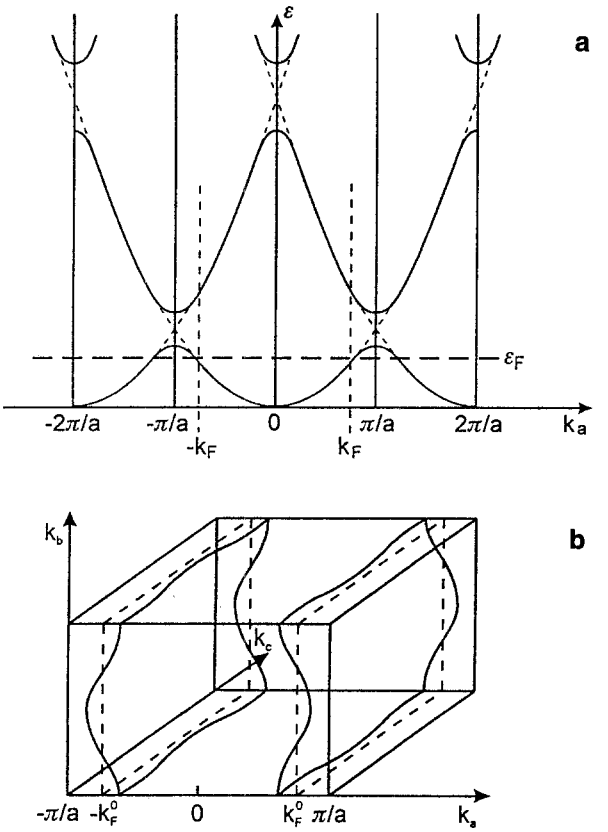

Fig. 2.2. (a) Schematic illustration of the free-electron-like 1D dispersion relation. ϵ_F is the Fermi energy, k_F is the Fermi wave vector, and a is the lattice constant. (b) 3D schematic view of the resulting Fermi surface. Dashed line without interstack overlaps. Solid lines with small transfer integrals

In the tight-binding band approximation the analogous result for the dispersion relation can be written as

$$\epsilon(\boldsymbol{k}) = 2t_a \cos(\boldsymbol{a}_\mathrm{m}\boldsymbol{k}) + 2t_b \cos(\boldsymbol{b}_\mathrm{m}\boldsymbol{k}) + 2t_c \cos(\boldsymbol{c}_\mathrm{m}\boldsymbol{k}), \tag{2.1}$$

where $\boldsymbol{a}_\mathrm{m}$, $\boldsymbol{b}_\mathrm{m}$, and $\boldsymbol{c}_\mathrm{m}$ are intermolecular distances in the crystal lattice directions a, b, and c, $\boldsymbol{k}$ is the electron wave vector, and t_i is the electron transfer energy along the i direction. For $(\mathrm{TMTSF})_2X$ both $\boldsymbol{b}_\mathrm{m}$ and $\boldsymbol{c}_\mathrm{m}$ correspond to the lattice constants b and c, while $\boldsymbol{a}_\mathrm{m} = a/2$ due to the dimerization of the TMTSF molecules (see Fig. 2.1). From plasma frequency measurements

[42] the transfer energies are estimated to $t_a \approx 0.28\,\mathrm{eV}$ and $t_b \approx 0.022\,\mathrm{eV}$. The transfer along the c direction is of the order 1 meV.

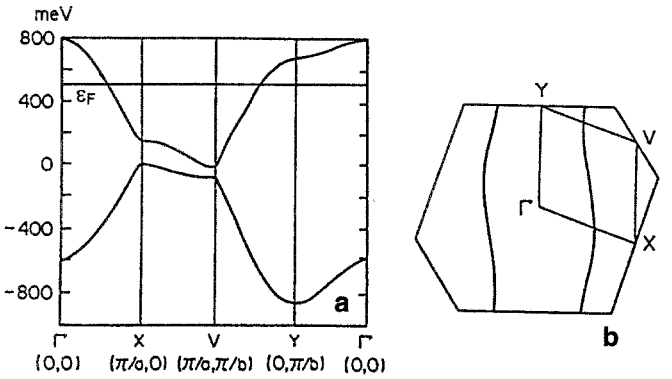

Fig. 2.3. (a) Calculated band structure and (b) Fermi surface of $(TMTSF)_2AsF_6$ representative for all $(TMTSF)_2X$. From [43]

Numerical tight-binding band-structure calculations result in the approximative dispersion relation which is valid in the neighborhood of the FS [43]

$$\epsilon(\boldsymbol{k}) \simeq 2[t_\mathrm{I} \cos(\boldsymbol{kb}) \pm t_\mathrm{S} \cos(\frac{1}{2}\boldsymbol{ka})], \tag{2.2}$$

where t_S and t_I are averaged transfer energies within the stacks and approximated interstack interactions in b direction, respectively. Because of the dimerization two bands ($\pm$) occur in the calculation. For $(TMTSF)_2PF_6$ the calculation results in $t_\mathrm{S} = 0.38\,\mathrm{eV}$ and $t_\mathrm{I} = 0.024\,\mathrm{eV}$. Therefore, in a first approximation the electronic band structure can be regarded as quasi 1D. The remaining dispersion along b, however, becomes important for charge and spin density wave phase transitions. Figure 2.3 shows the calculated band structure and the 2D FS of the first Brillouin zone of $(TMTSF)_2AsF_6$. For different anions the dispersion relation and the FS are almost indistinguishable [43]. Note the similarity of the dispersion relation along ΓX with the text-book free-electron picture of Fig. 2.2.

2.2.3 Ground-State Instability

Although the electronic system in the Bechgaard salt is quasi 1D the crystal lattice of course is three dimensional. Due to the strong anisotropy, however, the lattice has vibrational modes of very different energies. In addition, because of the weak coupling the organic crystals are not very rigid. This results, for example, in the peculiar so-called mechanical kink effect. By carefully pushing a point on the side of a thin needle-like crystal of $(TMTSF)_2ClO_4$ a pair of kinks along the long axis of the crystal can be produced [44]. These

kinks can be removed and even moved along the needle axis by appropriate local pressure treatment.

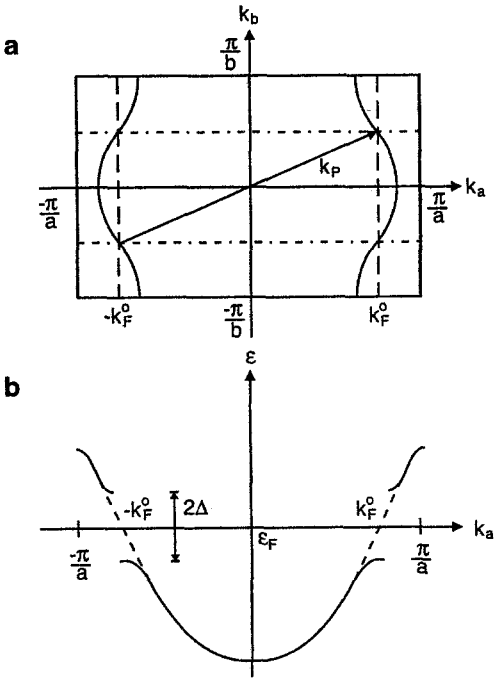

Fig. 2.4. (a) Schematic representation of a quasi 1D Fermi surface with nesting vector $\boldsymbol{k}_P = (2k_F, \pi/b, 0)$. The dash-dotted line is the resulting new Brillouin zone. (b) Opening of the Peierls gap 2Δ at $\pm k_F$ in the dispersion relation

The strong mutual interaction between the electronic system and the lattice of the Bechgaard salts is often seen in a combined lattice and electronic phase transition, the so-called Peierls instability. Metals with a pronounced 1D character are unstable against a perturbation with wave number $2k_F$, where k_F is the Fermi wave vector. Figure 2.4a shows schematically the 2D projection of a quasi 1D metallic FS with a cos-like modulation along k_b (see also Fig. 2.2b). As can be seen in Fig. 2.4a, the left sheet of the FS can be superposed on the right sheet of the FS by the translational vector $\boldsymbol{k}_P$. In other words it is said that the FS is nested by the vector $\boldsymbol{k}_P$. If now the lattice (or more generally an external field) modifies its structure with the nesting or Peierls wave vector, $\boldsymbol{k}_P$, a new Brillouin zone is generated (dashed lines in Fig. 2.4a) with $\boldsymbol{k}_P$ being exactly a reciprocal lattice vector. At this new zone boundary the energy of the electron levels will be reduced due to Bragg reflection, as shown schematically in Fig. 2.4b. For the case of complete FS nesting the whole FS disappears in the ground state. If some parts of the FS have different curvatures, i. e., higher dimensionality, the nesting will be

incomplete and parts of the FS will remain, eventually even as new closed parts.

Depending on the relative energies for the lattice distortion and the electron-energy redistribution the Peierls transition will occur. The critical temperature, T_P, can be calculated and is given by

$$k_B T_P = 1.13\,\epsilon_B \exp\left(-\frac{A_P}{\lambda^2}\right), \tag{2.3}$$

where k_B is the Boltzmann constant, ϵ_B specifies the energy region where the electron distribution is perturbed ($\gg k_B T$), λ is the electron–phonon coupling constant, and A_P is a material constant depending on the Fermi velocity, lattice constants and normal-mode frequencies. Below T_P, therefore, together with a lattice change an energy gap of 2Δ at ϵ_F will occur and the quasi 1D metal will become an insulator. Concomitant with the lattice modulation an electron density modulation occurs. As can be seen from the tangential form of the electron dispersion at the new Brillouin zone boundary, the electronic density of states is drastically enhanced at the wave vector $2k_F$. This transition, therefore, is often also called charge density wave (CDW) transition [45].

As first pointed out by Overhauser [46], the perturbing potential for the opening of a gap at the FS might also come from a spin redistribution. This so-called spin density wave (SDW) orders the spins of the itinerant electrons antiferromagnetically with the same nesting vector $\boldsymbol{k}_P$ as for the CDW. Below the corresponding transition temperature, T_M, the metal becomes insulating and an analogous gap at the FS is formed [47].

The occurrence of the energy gap 2Δ below the Peierls transition temperature allows in principle the collective motion of the electrons under the influence of an applied electric field. This holds as long as the energy $\hbar k_F v_{Fr}$ of the moving electrons is less than Δ, where v_{Fr} is the velocity of the collectively moving electrons. However, this so-called Fröhlich mode [4] is very sensitive to lattice imperfections because it is a true 1D movement.

For the case where the bandwidth or the warping, i. e., the transfer integral (t_b, respectively t_I in (2.2)), is small the Coulomb repulsion between the electrons becomes important. A limited screening of the electron charge in a narrow band due to restricted electron movement can lead to a localized electron lattice, a so-called Wigner crystal. This, in fact, has been observed in the strongly 1D material TTF–TCNQ where in addition to the $2k_F$ Peierls lattice distortion a $4k_F$ modulation was found [48, 49, 50]. The estimated value for the on-site Coulomb repulsion U in TTF–TCNQ is $U/4t_b \simeq 0.9$ extracted from the frequency dependence of the NMR relaxation time [51] and the susceptibility above the Peierls transition [52].

Many of the Bechgaard salts show at ambient pressure a metal–insulator transition, T_{MI}, around a few tens of K as can be seen from the resistivity behavior shown for several $(TMTSF)_2X$ salts in Fig. 2.5 [35]. This transition is

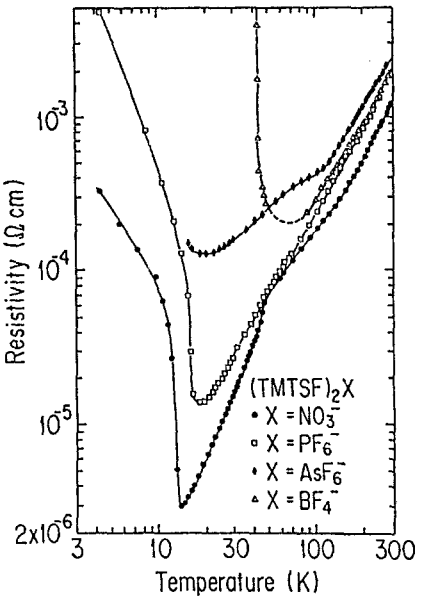

Fig. 2.5. Temperature dependence of the dc resistivity for various $(TMTSF)_2X$ salts in double-logarithmic scale. From [35]

neither accompanied by a lattice distortion nor by an isotropic decrease of the magnetic susceptibility. The latter effect should occur for a Peierls transition with a CDW, since then the carrier density should decrease exponentially with the opening of the gap Δ.

Measurements of the magnetic susceptibility, χ, below T_{MI} show a strongly anisotropic behavior. This can be seen in Fig. 2.6 where as an example χ of $(TMTSF)_2AsF_6$ is plotted [53, 54, 55]. For B parallel to a and c^* (= the direction perpendicular to both a and b) χ behaves similarly with a small anomaly around T_{MI} and a slight increase below the transition. For B parallel b' (= perpendicular to a and c^*) χ vanishes exponentially below T_{MI} (see inset of Fig. 2.6). This behavior is characteristic of an antiferromagnetically ordered state where the spin orientation is alternating along the b' direction. This kind of spin ordering is confirmed for $(TMTSF)_2AsF_6$ and also for $(TMTSF)_2PF_6$ both by ESR and NMR experiments [53, 56, 57, 58, 59]. The metal–insulator transition in $(TMTSF)_2X$ is, therefore, believed to be a SDW ordering. With ^{1}H NMR experiments it was even possible to estimate the SDW nesting vector $\boldsymbol{Q} = (Q_a, Q_b, Q_c)$, with $Q_a = 2k_{\mathrm{F}}$, $Q_b \simeq 0.2b^*$, and $Q_c \simeq 0$, and the amplitude $\sigma \approx 0.08\mu_{\mathrm{B}}$ of the SDW modulation, where μ_{B} is the Bohr magneton [60, 61]. The value of σ less than one means that the moments are not well localized but retain still an itinerant character. The vector $\boldsymbol{Q}$ is in good agreement with the nesting vector of the calculated band structure (see Fig. 2.3).

The large variety of ground states in quasi-1D organic conductors not only depends on the chemical composition of the organic molecule and the